Progress of Theoretical Physics, Vol. 85, No. 2, February 1991

Negative-Parity States of $N=88$ Isotones in the SDF Boson Plus a Fermion Pair Model

D. S. CHUU, S. T. HSIEH* and M. M. KING YEN**

Department of Electrophysics, National Chiao Tung University, Hsinchu, Taiwan
**Department of Physics, National Tsing Hua University, Hsinchu, Taiwan*
***Department of Nuclear Engineering, National Tsing Hua University Hsinchu, Taiwan*

(Received July 28, 1990)

The energy levels of negative parity states of $N=88$ isotones: ^{158}Yb, ^{156}Er and ^{154}Dy are studied in terms of the SDF interacting boson approximation (IBA) model with one s- or d-boson being able to break and form a fermion pair. The fermion pair is allowed to occupy the $i_{13/2}$ single particle orbit. It is found that the energy levels of the negative parity bands of these nuclei can be reproduced satisfactorily. The backbends of the moment of inertia can be also reasonably described.

§ 1. Introduction

The interacting boson approximation (IBA) model[1] has been successful to describe the low-lying collective states in many medium to heavy even-even nuclei. Recently, the deformed nuclei with $N\simeq 90$ and $64<Z\leq 70$ have received considerable attention.[2)~13)] The $N=88$ nuclei, lying just outside the permanently deformed region which begins at $N=90$, are expected to be soft with respect to shape changes.[2),5),8),9)] Recently, a large amount of experimental studies[5)~12)] had identified some high-spin negative parity odd and even bands existing in the $N=88$ nuclei. Among these data, the anomalous negative parity bands have been observed and the phenomena of backbending occurs as one plots the moment of inertia versus the square of the angular velocity for yrast band of a nucleus. Similar situations occur in the positive parity bands of these nuclei and many efforts[10)~17)] within the framework of IBA have been attempted to understand the mechanism of the sudden change of the behavior of the moment of inertia for the positive parity bands. It is generally believed that the high spin anomalies are produced by the complicated interplays between the collective and the single-particle degrees of freedom induced by the Coriolis decoupling. The backbending phenomena and anomalous negative parity bands of ^{156}Er have been studied in the two-quasiparticle plus rotor bandmixing model.[18)] In this model the high spin states are produced by the alignments of the angular momenta of the decoupled quasiparticles along the collective rotation, and the observed backbends are attributed to the intersection of the zero-quasiparticle band and the decoupled two-quasiparticle band. Hence, it will be interesting to see to what extent the extended IBA model is able to describe the structures of the negative parity bands.

In this work we shall study high spin negative parity bands by incorporating the traditional interacting sd-boson model with one f-boson (sdf IBA) and allow one s- or d-boson to have the fermion pair degree of freedom. To make the calculation feasible, we include only one f-boson and consider only one single particle orbit. The

low spin states are excluded from the calculation to avoid the inclusion of the p-boson in our model space. In the region of well-deformed nuclei the unique parity intruder orbitals such as $h_{11/2}$ and $i_{13/2}$ are generally believed to be the most important because both the Coriolis antipairing effect and the rotation alignment effect increase with increasing angular momentum.[13),14)] However, a recent study on the positive parity high-spin states of $N=88$ isotones manifested that the orbit $i_{13/2}$ is the most important one for the first backbending.[17)] Therefore, as a first exploration of the model, we may restrict to this orbit only. Our model will be applied to study the negative parity bands of $N=88$ isotones: ^{158}Yb, ^{156}Er and ^{154}Dy. These nuclei are all well known for the structure change at high spin,[2),5),8),9)] and their abundant negative parity bands provide a good testing example of the extended IBA model. The IBA model including one f- or one p- boson in the calculation has been previously applied to study the negative states of $N=88$ isotones.[19)] It was found that states below $I\simeq 20$ can be reproduced well.

§ 2. The model

The $N=88$ isotones: ^{158}Yb, ^{156}Er and ^{154}Dy will be taken as testing examples. Thus, valence protons and valence neutrons are in the 50-82 and 82-126 major shell respectively. Taking $Z=N=82$ as the core, pure IBA assumes a valence s- and d-boson number $N_B=8$, 9 and 10 plus an f-boson for the three nuclides, ^{158}Yb, ^{156} Er and ^{154}Dy, respectively. In addition to the pure boson configuration, we admix the N_B-1 sd-boson and one f-boson plus one fermion pair configuration into the model space. To be more specific, the model space is spanned by two types of basis states,

$$|n_s n_d \nu a L, f;\ L_T M_T\rangle$$

and

$$|[n_s' n_d' \nu' a' L', j^2(J)]L_c, f;\ L_T M_T\rangle\,,$$

where $n_s+n_d=N_B$, $n_s'+n_d'=N_B-1$, $j=13/2$ and $J\geq 4$. The total boson number is $N=N_B+1$. The $J=0$ and 2 fermion pair states are excluded to avoid double counting of the states.

The model hamiltonian consists of four parts:

$$H=H_B+H_F+V_{BF}+V_N\,,$$

where H_B is the IBA boson hamiltonian

$$H_B=a_0 n_d+a_1 P^\dagger P+a_2 L\cdot L+a_3 Q\cdot Q\,.$$

The octupole term $T_3\cdot T_3$ and the hexadecapole term $T_4\cdot T_4$ have been omitted in H_B since they are generally believed to be less important. The fermion hamiltonian H_F is

$$H_F=\sum_m \varepsilon_j a_{jm}^\dagger a_{jm}+\frac{1}{2}\sum_J V^J(a_j^\dagger a_j^\dagger)^J\cdot(\tilde{a}_j\tilde{a}_j)^J\,,$$

where ε_j is the fermion single particle energy, the V^J's are the fermion-fermion

interactions, and $a_j^\dagger$ ($\tilde{a}_j$) is the nucleon creation (annihilation) operator. The mixing hamiltonian V_{BF} between the *sd* boson and the fermion is assumed

$$V_{BF}=aQ^B\cdot(a_j^\dagger\tilde{a}_j)^{(2)}+\beta Q^B\cdot[(a_j^\dagger a_j^\dagger)^{(4)}\tilde{d}-d^\dagger(\tilde{a}_j\tilde{a}_j)^{(4)}]^{(2)},$$

where

$$Q^B=(d^\dagger\tilde{s}+s^\dagger\tilde{d})^{(2)}-\sqrt{7}/2(d^\dagger\tilde{d})^{(2)},$$

and the Hamiltonian related to the *f*-boson part is

$$V_N=\varepsilon_f n_f+\gamma Q^B\cdot(f^\dagger\tilde{f})^{(2)}+\delta(a_j^\dagger\tilde{a}_j)^{(2)}\cdot(f^\dagger\tilde{f})^{(2)}$$

which includes the *f*-boson single particle energy and the mixing hamiltonian of *f*-boson with the *sd*-boson, and with the fermion. In the calculation, the radial dependence of the fermion potential is taken as the Yukawa type with a Rosenfeld mixture. An oscillation constant $\nu=0.96\,\mathrm{A}^{-1/3}$ fm^{-2} with $A=160$ is assumed. The interaction strengths of the V^J's are determined by requiring:

$$\langle jj|V|jj\rangle_{J=2}-\langle jj|V|jj\rangle_{J=0}=2\ \text{MeVs for}\ j=13/2\,.$$

The single particle energy ε_j ($j=13/2$) is obtained as a result of fitting. The other parameters contained in the boson hamiltonian H_B, V_N and V_{BF} were chosen to reproduce the negative parity energy spectra of ^{158}Yb, ^{156}Er and ^{154}Dy isotones respectively. The ε_f is set to be zero because all the states considered in our calculation contain one *f*-boson. In the calculation the interaction parameters contained in the boson part for each nuclei are kept to be the same values for either the N boson configuration or the $N-1$ boson plus a fermion pair configuration. The interaction strengths and the single particle energies for each isotone are allowed to be mass number dependent.

§ 3. Results

Table I presents the final searched values of the interaction strengths and single particle energies. The mixing parameters α, β, γ and δ can be unified as (in MeV): $\alpha=0.21$, $\beta=0.025$, $\gamma=-0.015$ and $\delta=0.15$. The energy level fitting can be improved slightly if we use a non-unified set of α, β and γ for different nuclide whilst the other parameter δ is more or less insensitive to the energy level fitting. The smallness of the mixing parameters manifests the fact that the mixings between the pure boson configuration and the configuration with one fermion pair are small. The strength of

Table I. The interaction parameters in MeV for IBA plus one fermion pair model.

parameter (MeV)	N_B	a_0	a_1	a_2	a_3	$\varepsilon_{13/2}$
^{158}Yb	8	0.1404	−0.041	0.0079	−0.0057	1.758
^{156}Er	9	0.1103	−0.051	0.0083	−0.0036	1.725
^{154}Dy	10	0.0585	−0.053	0.0098	−0.0029	1.689

the d-boson energy a_0 and the single fermion energy for the $i_{13/2}$ orbit decrease while the parameter a_2 of the $L\cdot L$ term increases as boson number increases. This corresponds to the fact that the isotones become more collective as the boson number increases. This is consistent with the tendency of deviating away from $U(5)$ symmetry to become the $O(6)$ and $SU(3)$ symmetry. The strength parameters of the pairing term $P^\dagger\cdot P(a_1)$ and the quadrupole term $Q\cdot Q(a_3)$ are negative. The former grows with mass number and the latter behaves just oppositely.

Energy levels calculated using these parameters are compared with actual data. For ^{158}Yb, abundant negative parity levels were observed recently.[5)~7)] Three negative parity bands have been established by Patel et al.[7)] using twenty-one Compton-suppressed germanium detectors of the Hera array. They are plotted on the left-hand side of Fig. 1. To make comparison more clearly, we display the different quasibands in different columns. Between the main odd-spin band and the even-spin band there is another very short even band which consists of four second states: 10_2^-, 12_2^-, 14_2^- and 16_2^-. The nature of this band is not very clear now. It can well be νBE configuration,[7)] where as in the usual shell-model assignments, B is one of the lowest-lying (mixed) configurations based on the unique-parity orbits $i_{13/2}$ for neutron (ν) and $h_{11/2}$ for proton (π), and E is one of the lowest-lying normal-parity neutron configurations based on mixed $f_{7/2}$ and $h_{9/2}$ orbitals. Assume this band consists of all second states for each even spin, then our calculation yields predictions for those yet unobserved band components. It is shown on the right-hand side of Fig. 1. For all

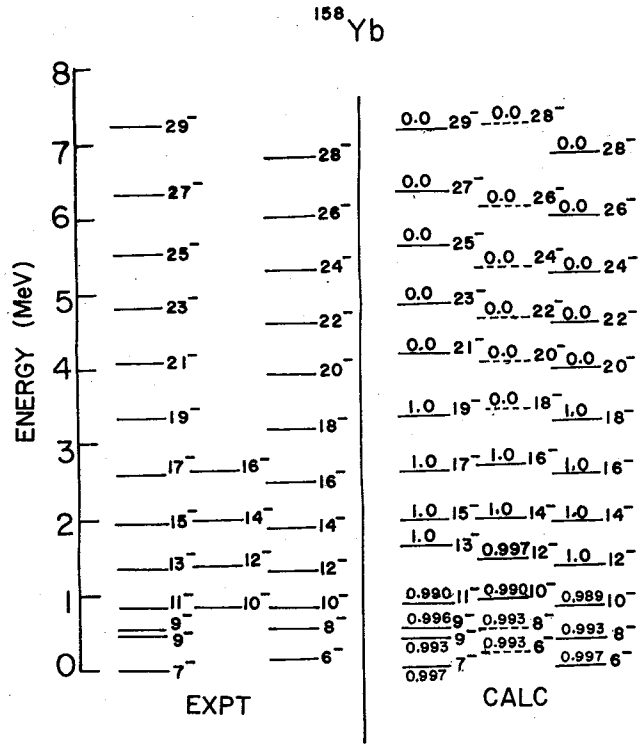

Fig. 1. The calculated and observed negative parity energy spectra for ^{158}Yb. The observed data are taken from Refs. 5)~7). The levels in dashed lines are the predicted energy levels.

observed energy levels the agreement between the calculated and the observed spectra are rather good, including the two closely spaced 9^- levels. The number right above each energy level is extracted from the calculated wavefunction of that particular level. It is the intensity of the pure *sdf* boson configuration. Since most of the levels are rather pure, one can see that starting from $I\sim 20$ the *sdf*-boson-plus-two-fermions configuration supersedes the pure boson configuration. This appears to be true for all three bands.

The level scheme of ^{156}Er has been determined[8] recently using an array of nine Compton-suppressed Ge detectors. Five bands and pieces of two or three other bands have been observed. Among these bands there are three long negative parity bands (two odd bands and one even band) and one piece of negative odd spin band which contains only three levels 19_2^-, 21_2^- and 23_3^- as shown on the left-hand side of Fig. 2. If we assume that the lower part ($I\leq 21$) of this short band consists of second levels of odd spin; and the upper part ($I>21$) consists of third levels of odd spin, then the calculated results are shown on the right-hand side of Fig. 2 with pure boson intensity indicated on each level. In terms of spectra, the comparison between the two sets is again rather good. Evidence for structure change in ^{156}Er is found[8] in the intense feeding among four negative parity bands. One can note from Fig. 2 that the states with $I\leq 19$ of the yrast negative parity odd spin band for the nucleus ^{156}Er are essentially the pure boson configuration while the states with higher angular momentum are definitely the one fermion pair excitation configuration. The 19_2^- and 23_3^- states contained in the piece of the negative parity odd spin band are pure states of

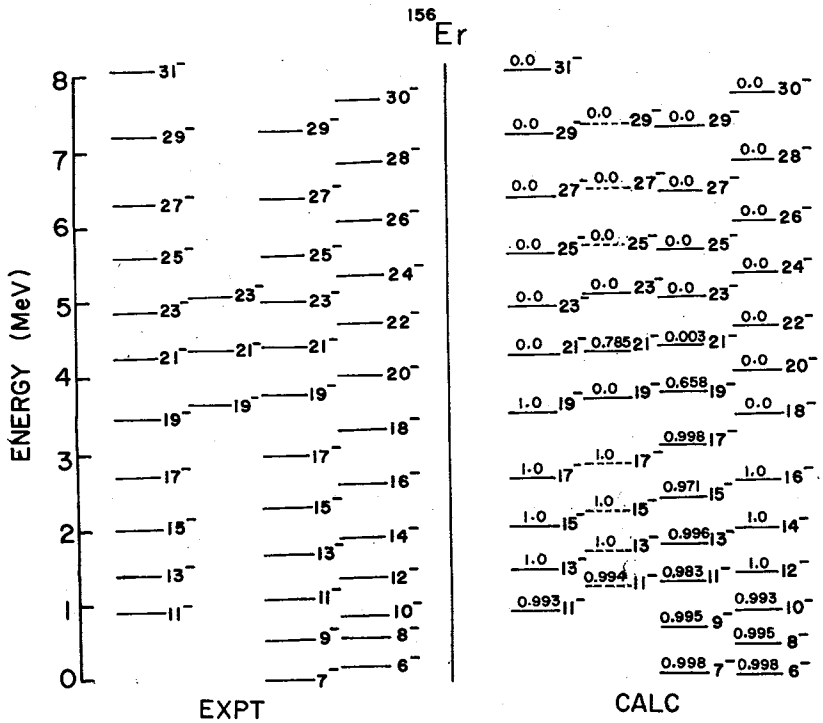

Fig. 2. The calculated and observed negative parity energy spectra for ^{156}Er. The observed data are taken from Ref. 8). The levels in dashed lines are the predicted energy levels.

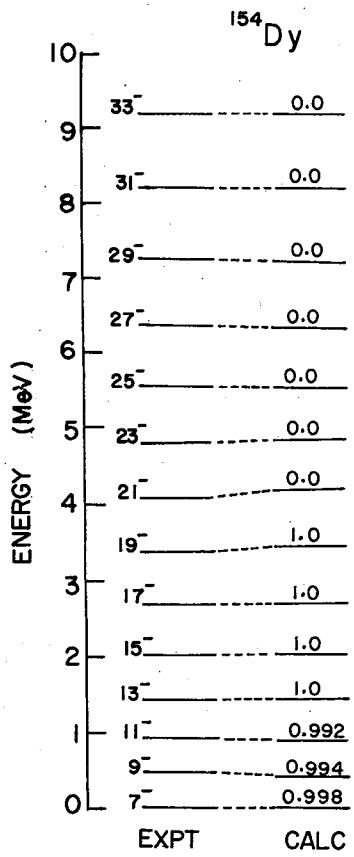

Fig. 3. The calculated and observed negative parity energy spectra for ^{154}Dy. The observed data are taken from Refs. 9)~12).

$N-1$ plus one fermion pair configuration while the 21_2^- state is a mixed state. In the other odd spin band of ^{156}Er, the $N-1$ boson plus one fermion pair configuration takes over at $I=21$. In the even band, this happens at $I=18$. The mixing between two configurations is in general very small except for the two odd spin states: 19_3^- (65.8 %) and 21_2^- (78.5 %).

There are abundant experimental data observed for ^{154}Dy in the recent years.[9)~12)] The negative parity states of ^{154}Dy from 9^- up to 37^- were assigned definitely.[10)] The calculated and the observed energy spectra for ^{154}Dy are shown in Fig. 3. It can be seen from Fig. 3 that the energy levels of ^{154}Dy can be reproduced quite well. Level wavefunctions reveal that lower states with $I \leq 19$ are essentially the pure boson configuration while the states with $I>19$ are definitely the $N-1$ boson plus one fermion pair configuration. In a previous study of the discrete levels in ^{154}Dy above $I=30$, Cranmer-Gordon et al.[10)] suggested the $I\sim20$ discontinuity is caused by an alignment of two $i_{13/2}$ quasineutrons within a band. Our result seems to be consistent with the conclusion of Ref. 10). The apparent variations for the intensities of different configurations

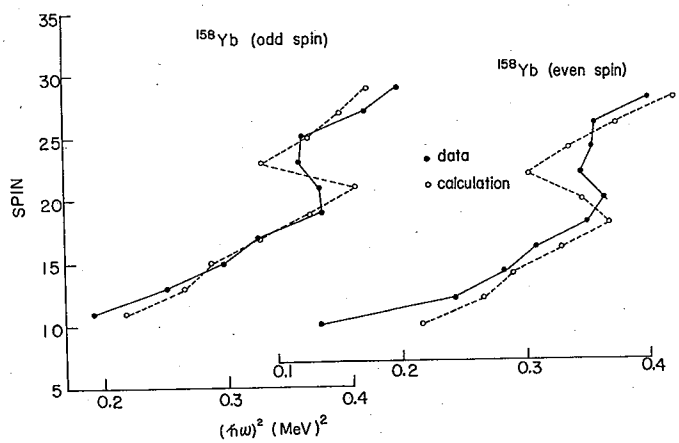

Fig. 4. The calculated and observed spin angular momentum I vs $(\hbar\omega)^2$ for negative parity odd and even spin states of ^{158}Yb.

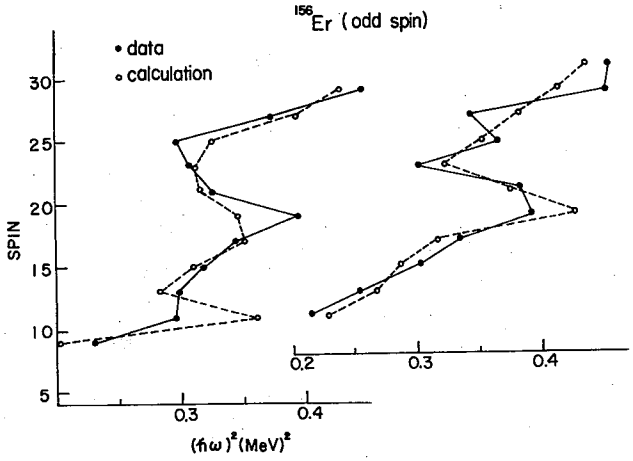

Fig. 5. The calculated and observed spin angular momentum I vs $(\hbar\omega)^2$ for negative parity odd spin states of ^{156}Er.

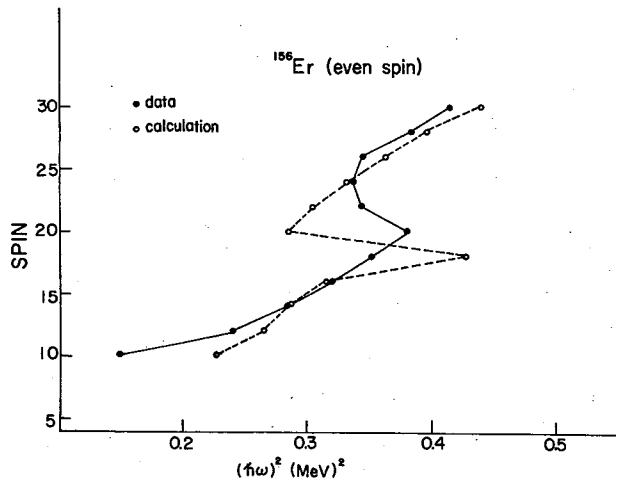

Fig. 6. The calculated and observed spin angular momentum I vs $(\hbar\omega)^2$ for negative parity even spin states of ^{156}Er.

with the angular momenta in these three isotones manifest that two bands of different deformations are crossing each other around $I\sim20$.

Figures 4~7 show the calculated and the observed backbending plots for these three isotones. The odd spin band and the even spin band are displayed in separate figures. Here we choose the sensitive expression as to plot the angular momentum I vs $(\hbar\omega)^2$ curves, with

$$(\hbar\omega)^2=\left\{\frac{E_{I+2}-E_I}{[I(I+1)]^{1/2}-[(I-2)(I-1)]^{1/2}}\right\}^2.$$

The backbending curve of the negative parity odd and even bands for ^{158}Yb are shown in Fig. 4. One can see from Fig. 4 that the observed backbend occurs at spin $I=19$ for the odd band whereas in the calculated band it occurs at $I=21$. However, the main feature can still be reproduced reasonably in our model. The backbend occur-

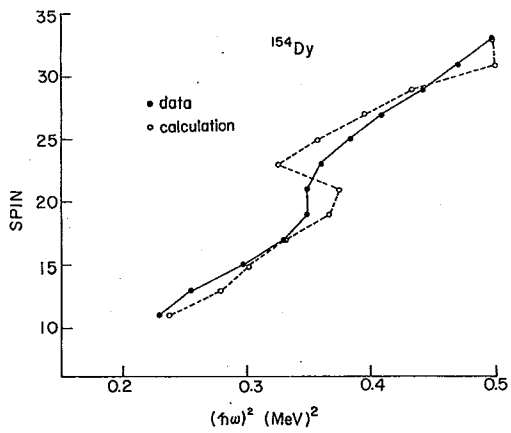

Fig. 7. The calculated and observed spin angular momentum I vs $(\hbar\omega)^2$ for negative parity states of ^{154}Dy.

ring at spin $I=18$ for the even band is overly reproduced. Therefore, the backbend curve of the negative even band at higher spin cannot be reproduced satisfactorily in the present model. The same situation occurs in the previous calculation of the positive parity bands of $N=88$ isotones.[17] The backbending curve of the odd and even negative parity bands for ^{156}Er are shown in Figs. 5 and 6 respectively. From Fig. 5, we find that our calculated curves imitate the data overly. The left one somewhat exaggerates the backbend at 11^- and bends too early at 17^- and 23^-. The right one reproduces data curve nicely except at high spins. For the even band shown in Fig. 6, the calculated curve bends too early and too drastically. Figure 7 shows the backbending curve of the negative parity band for ^{154}Dy. One can see from the figure that the calculated curve agrees reasonably with the observed one. Except for the fine variations near the backbend, the main feature of the observed data for these nuclides can be reproduced satisfactorily. In order to explain the detailed variations existing at the higher spins some additional mechanism such as more single particle orbits or more fermion pairs should be considered.

§ 4. Summary and discussion

In summary we have investigated the structure of the negative parity energy spectra and the backbending phenomena of the isotones ^{158}Yb, ^{156}Er and ^{154}Dy. We extend the IBA model to include an f-boson to substitute for an sd-boson and allow an sd-boson to break into a fermion pair which can occupy the $i_{13/2}$ orbit. The calculated energy levels including the negative parity even spin and odd spin bands are all in satisfactory agreement with the observed values for these three isotones. We also plot the backbending curve of the negative odd spin and even spin bands for ^{158}Yb and ^{156}Er and the yrast negative parity band for ^{154}Dy. The observed data are able to be satisfatorily explained. The effect of the introduction of the fermion pair degrees of freedom manifested in the improvement of the calculated energy levels and the variations in the calculated backbending curves when we compare with the previous result.[19] The couplings to angular momenta $J=4, 6, 8, \cdots$ for the fermion pair in $i_{13/2}$ orbit may be considered as implicitly including the higher angular momentum bosons, such as g-boson and the i-boson, $\cdots$ etc., and therefore making the IBA model space more complete. This is also manifested in the analysis of the wavefunctions. The high spin states are usually dominated by the $N-1$ boson plus one fermion pair configuration and thus cannot be reproduced by the traditional IBA model. The fine variations occurring in the backbending curve of the odd spin band

for ^{156}Er might be hopefully interpreted by considering more single particle orbits or more *sd*-bosons to break into fermion pairs and make more band crossings to form the fine variations in the backbending curves.

This work is supported by the National Science Council of ROC.

References

1) A. Arima and F. Iachello, Phys. Rev. Lett. **35** (1975), 1069; **40** (1978), 385; Ann. of Phys. **99** (1976), 253; **111** (1978), 201; **121** (1979), 468.
2) A. L. Goodman, Phys. Rev. **C39** (1989), 2008; **39** (1989), 2478.
3) J. B. Gupta, Phys. Rev. **C49** (1989), 1604.
4) D. R. Zolonowski, M. B. Hughes, J. Hunt and T. T. Sugihara, Phys. Rev. **C21** (1980), 2556.
5) I. Ragnarsson, T. Bengtsson, W. Nazarewicz, J. Dudek and G. A. Leander, Phys. Rev. Lett. **54** (1985), 982.
6) C. Baktash, Y. Schutz, I. Y. Lee, F. K. Mcgowan, N. R. Johnson, L. Courtney, A. J. Larabee, L. L. Riedinger, A. W. Sunyer, E. der Mateosian, O. C. Kistner and D. G. Sarantites, Phys. Rev. Lett. **54** (1985), 978.
7) S. B. Patel, F. S. Stephens, J. C. Bacelar, E. M. Beck, M. A. Deleplanque, R. M. Diamond and J. E. Draper, Phys. Rev. Lett. **57** (1986), 62.
8) F. S. Stephens, M. A. Deleplanque, R. M. Diamond, A. O. Macchiavelli and J. E. Draper, Phys. Rev. Lett. **54** (1985), 2584.
9) A. Pakkanen, Y. H. Chung, P. J. Daly, S. R. Faber, H. Helppi, J. Wilson, P. Chowdhury, T. L. Khoo, I. Ahmad, J. Borggreen, Z. W. Grabowski and D. C. Radford, Phys. Rev. Lett. **48** (1982), 1530.
10) H. W. Cranmer-Gordon, P. D. Forsyth, D. V. Elenkov, D. Howe, J. F. Sharpey Schafer, M. A. Riley, G. Sletten, J. Simpson, I. Ragnarsson, Z. Xing and T. Bengtsson, Nucl. Phys. **A465** (1987), 506.
11) F. Azgui, H. Emling, E. Grosse, C. Michel, R. S. Simon, W. Spreng, T. L. Khoo, P. Chowdhury, D. Freker, R. V. F. Janssens, A. Pakkanen, R. J. Daly, M. Kortelahti, D. Schwalm and G. Seiler-Clark, Nucl. Phys. **A439** (1985), 573.
12) R. Holzmann, T. L. Khoo, W. C. Ma, I. Ahmad, B. K. Dichter, H. Emling, R. V. F. Janssens, M. W. Drigert, U. Garg, M. A. Quader, P. J. Daly, M. Piiparinen and W. Trzaska, Phys. Rev. Lett. **62** (1989), 520.
13) N. Yoshida, A. Arima and T. Otsuka, Phys. Lett. **114B** (1982), 86.
14) N. Yoshida and A. Arima, Phys. Lett. **164B** (1985), 231.
15) C. E. Alonso, J. M. Arias and M. Lozano, Phys. Lett. **177B** (1986), 130.
16) D. S. Chuu and S. T. Hsieh, Phys. Rev. **C38** (1988), 960.
17) M. M. King Yen, S. T. Hsieh and H. C. Chiang, Phys. Rev. **C38** (1988), 993.
18) C. Flaum and D. Cline, Phys. Rev. **C14** (1976), 1224.
19) C. S. Han, D. S. Chuu, S. T. Hsieh and H. C. Chiang, Phys. Lett. **163B** (1985), 259.